

# THE DYNAMIC TRANSMISSION MAP FOR DEHAZING METHOD IN SINGLE IMAGE WITH TROPICAL ATMOSPHERIC CONDITION

<sup>1</sup>NOOR ASMA HUSAIN, <sup>2</sup>MOHD SHAFRY MOHD RAHIM, <sup>3</sup>SARUDIN KARI, <sup>4</sup>ABDULLAH BADE, <sup>5</sup>HUMA CHAUDHRY

<sup>1,2</sup>School of Computing, Faculty of Engineering, Universiti Teknologi Malaysia

<sup>3,4</sup>Faculty of Science and Natural Resources, Universiti Malaysia Sabah

<sup>5</sup>College of Engineering and Science, Victoria University, Melbourne, Australia

E-mail: <sup>1</sup>nasma4@live.utm.my, <sup>2</sup>shafry@utm.my, <sup>3</sup>sarudin@ums.edu.my, <sup>4</sup>abb@ums.edu.my,

<sup>5</sup>huma.bicse@gmail.com

## ABSTRACT

Normally, outdoor images are degraded by light scattering and absorption from the atmosphere's dust, mist, haze, and smoke. These affect the image captured and cause poor visibility, dimmed luminosity, low contrast, and colour distortion. Therefore, it is crucial to restoring images captured, especially in haze conditions called image dehazing. The crucial aim of image dehazing is to improve the details on visibility, edge, and texture and retain the structure and colours of the image without data loss. Most algorithmic methods, considering the large number of algorithms suggested for single image dehazing, introduce dehazing at a certain haze level. There is a lack of a dehazing algorithm focused on the visibility range to overcome several haze levels. This paper proposes an improvement of the dehazing algorithm based on the meteorological visibility range with a dynamic transmission map to fix this problem. This algorithm focuses on removing haze at different levels based on the determination of the visibility range, which is different from most existing dehazing algorithms. The dehazing algorithm emphasizes this proposed method contribute to better image quality than the existing state-of-the-art dehazing process.

**Keywords:** *Haze, Atmospheric Scattering Model, Image Dehazing, Scattering Coefficient, Transmission Map*

## 1. INTRODUCTION

The atmospheric phenomena of haze, fog, and mist are all attributed to contaminants such as dust, sand, water droplets, or ice crystals from the atmosphere. These phenomena in meteorology mainly vary due to material, scale, shape, and concentration. Their physical effects on images, however, are identical. The haze appears to create a distinctive hue of grey or bluish and affects visibility [1]. Haze is an estimated degradation found in outdoor images especially for applications of computer vision, where image contrast decreases as particles suspended in the air disperse the light. This condition induces low contrast and poor picture visibility. The haze-induced loss of information makes images visually unattractive and poses challenges for both human and machine

vision, making it difficult to identify, track or navigate objects [2,3].

Koschmieder suggested a haze-explained atmospheric scattering model in which horizontal airlight dispersion and reflection and propagation-based attenuation led to the low quality of the image [4]. Between the camera sensor and the captured object, the contributions control the optical thickness of the media. The direct transmission from the scene to the camera is decreased by scattering and absorption, introducing another layer of the ambient scattered light, known as airlight, as shown in Figure 1. The attenuated direct transition causes the strength of the scene to be lower, and the airlight causes the appearance of the scene to be washed out. There has been a substantial improvement in previous studies in approaches that use photographs captured in hazy scenes. Atmospheric signals are used by Cozman and

Krotkov [5] and Nayar and Narasimhan [1] to estimate depth. Since then, many explicit visibility enhancement methods have been implemented, which can be grouped into four categories: multi-image methods [6], filter-based polarization methods [7], methods using proven depth or geometry [8], and single-image methods [9-19].

Most of the dehazing algorithms for single images have recently introduced various approaches to restore the hazy appearance to become a natural haze-free image. All researchers established multiple methods on a similar principle; to recover the clean scene from the haze. The key is to estimate an accurate medium of transmission map. In Tan [9] and Fattal [10], a breakthrough was made in improving single-image visibility, which can automatically dehaze a single image without additional information, such as known geometric information or user feedback. The drawbacks of the system are the presence of the halo around the discontinuation of depth due to the local window-based activity. In early work, Tan was given a less reliable estimate. In certain other instances, Fattal is not stable, and it obtains an accurate estimation when obtaining the most massive error. Fattal works well only at low levels of haze, and at medium and high levels of haze, the output decreases. He discovered that most outdoor items have at least one colour channel that is substantially dark in clear weather [11]. Computation time is one of the disadvantages of the techniques. For real-time applications where the depth of the input scenes varies from frame to frame, the procedures cannot apply. Tarel and Hautiere [12] introduce a fast visibility restoration method whose complexity is linear to the number of image pixels.

Meng [13] extends the dark channel's idea before determining the initial transmission values by introducing its lower bound. He and Meng also slightly underestimate the transmission because they essentially predict the lower bound of transmission. He and Meng's estimation becomes more accurate when the haze level increases. Ancuti proposes a method based on image fusion results in colour distortion [14]. Fattal introduces another approach based on colour lines but having low brightness [15]. Tang provides a framework focused on learning. Multi-scale characteristics such as dark channel [16], maximum local contrast, hue disparity, and maximum regional saturation are gathered from the process. To learn the association between the features and the transmission, it uses the random forest regressor.

Color Attenuation Prior (CAP) is suggested by Zhu, which relies on the difference between the saturation and the brightness of the hazy image pixels. In particular, the transmission depth was demonstrated by the use of colour attenuation for model parameters prior to a supervised learning process [17]. Cai [18] suggests a Tang-like learning-based system that trains a regressor to predict the value of the transmission from its surrounding patch. However, with the correct atmospheric light colour, the learning-based techniques depend heavily on the white balance stage. Once there are minor errors in the measurement of ambient light colour, their output drops rapidly. Berman [19] suggests an algorithm based on a previous modern non-local one. At a medium haze level, Berman can achieve the least transmission estimation error, but the error increases at both low and heavy haze levels.

Most of the dehazing method had solved haze problems with a certain haze level on a different range of real or synthetic haze images. The method's efficiency is different at the lower haze thickness to the highest level of haze thickness. In this paper, an enhanced dehazing algorithm known as Dynamic Transmission Map for Dehazing Method has been proposed, which has removed haze using four different haze levels with the dynamic transmission map.

## 2. ATMOSPHERIC SCATTERING MODEL

In the atmospheric scattering model proposed by Koschmieder, it has two appliances, which are direct attenuation,  $J(x)t(x)$ , and airlight,  $A(1-t(x))$ , as shown in Figure 1.

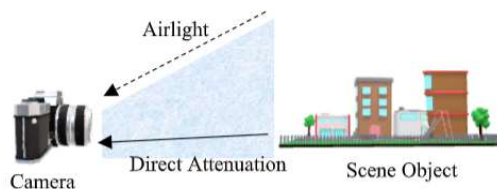


Figure 1: Atmospheric Scattering phenomena

Haze algorithm combined these appliances, given by [3], as follows:

$$I(x) = J(x)t(x) + A(1 - t(x)) \quad (1)$$

where  $I(x)$  represent a haze image,  $J(x)$  represents a haze-free image,  $t(x)$  represents direct transmission, and  $A$  is the airlight.

## 2.1 Airlight

In addition to light from a source objects that passes through the medium and is transmitted to the camera, ambient illumination in the atmosphere is often dispersed towards the camera by the same particles.

The most haze-opaque pixel has been used to estimate air-light in early work. The brightest pixel [9] was selected by Tan. For an optimization query, Fattal [10] used it as an initial guess. However, rather than air-light, the pixel with the greatest intensity could correspond to a bright object. He et al. [11] therefore suggest selecting the brightest pixel among the pixels with the top brightest values of the dark channel. This approach is useful and usually produces reliable results, but it assumes that the sky or another region is visible in the image without objects in line-of-sight.

White-balance is worked out by Tarel and Hautiere, and pure white (1, 1, 1) [12] is believed to be the air-light in RGB value. Sulami et al. [20] estimate the magnitude and direction of air-light separately. By searching for small patches with continuous transmission and surface albedo, the path is estimated. This is used by Bahat and Irani [21] until variations between such co-occurring patches are identified and air-light measured. To estimate the air-light [22], Berman uses a Hough transform. Hough transform is a useful technique via a voting scheme to detect unknown parameters of a model given noisy data.

## 2.2 Transmission Map

The most difficult part is the calculation of transmission maps  $t(x)$  between the radiance of the camera and the scene. The distance  $d(x)$  from the camera observer is the point of a scene. The transmission of haze is found to be physically linked to depth. Depth estimation is an important but challenging issue in computer vision [23].

$$t(x) = e^{-\beta d(x)} \quad (2)$$

Direct transmission is formulated by the atmospheric scattering coefficient,  $\beta$ , the distance or depth of the scene,  $d$ , between the observer and the target object [4]. It is worth noting that the most significant information is the depth of the scene. Since the scattering coefficient,  $\beta$ , can be regarded as a constant homogeneous state of the atmosphere, if the depth is given, the medium transmission,  $t(x)$  can be easily calculated according to Equation (2). In scalar [0,1],  $t(x)$

represents a transmission map. Some issues, such as halo artefacts, may result in an incorrect estimate of the transmission map. For this reason, several approaches to further refinement of transmission have been established.

The hazy image can be restored to a haze-free appearance,  $J(x)$ , once the airlight and the transmission map have been calculated, by using Equation (3) as given by Koshmieder [4]:

$$J(x) = \frac{I(x)-A}{t(x)} + A \quad (3)$$

Equation 3 shows the formula from Equation 1 to restore a hazy image based on estimated transmission and airlight. Most dehazing approaches used this formula, and they proposed various techniques to obtain a transmission map instead of directly used the scattering coefficient itself. This paper improved the dehazing method by suggesting a dynamic scattering coefficient in our methodology that explains in the next section.

## 3. METHODOLOGY

This section explains the research framework in Figure 2 for the proposed dehazing algorithm. This dehazing algorithm is mainly calculated by applying the atmospheric scattering model in Equation (1). The pre-processing for this process uses gamma correction applied to the hazy input image. Airlight estimation is done by Quadtree Decomposition on the corrected image brightness. Subsequently, scene depth estimated with Dark Channel Prior is used in measuring haze thickness. Based on the estimated scene depth, we compute mean value to obtain the suitable scattering coefficient value,  $\beta$ , based on the hazy image's visibility range. The visibility range estimation with a new visibility scale within intensity value [0,1]. A visibility scale is an improvement in this framework to yield a dynamic transmission map. Therefore, the visibility scale manages to determine a suitable scattering coefficient,  $\beta$  based on mean value measurement.

Table 1: The Weather Conditions Visibility Range and Its Scattering Coefficient [2]

No.	Weather Condition	Visibility Range, km	Scattering Coefficient, $\beta$
1	Dense Fog	< 50 m	>78.2
2	Thick Fog	50 m – 200 m	78.2 – 19.6
3	Moderate Fog	200 m – 500 m	19.6 – 7.82
4	Light Fog	500 m – 1000 m	7.82 – 3.91
5	Thin Fog / Dense Haze	1 km – 2 km	3.91 – 1.96
6	Haze	2 km – 4 km	1.96 – 0.954
7	Light Haze	4 km – 10 km	0.954 – 0.391
8	Clear	10 km – 20 km	0.391 – 0.196

9	Very Clear	20 km – 50 km	0.196 – 0.078
10	Exceptionally Clear	>50 km	0.078
11	Pure Air	277 km	0.0141

The scattering parameter  $\beta$  depends on the weather condition as in Table 1. Specifically, this scattering parameter is obtained from the visible range,  $R_m$ , via the relation  $\beta = \frac{-\ln(\epsilon)}{R_m}$  [23,24]. The contrast threshold  $\epsilon$  is set as 0.02. The new visibility scale referred to Table 1 to determine the scattering coefficient based on visibility range mapping.

Next, the transmission map estimation as in Equation (2) was derived based on the scattering coefficient and depth map parameter. The transmission value and airlight value were included in Equation (3) to yield a dehazed image. The post-processing of this process utilizes image enhancement, which is contrast stretching. The dehazed images evaluate using image quality assessments: MSE, PSNR, and SSIM and benchmarking against the ground truth image. The dehazing code is programmed using MATLAB 2017b with a CPU (Intel i5 7200, 2.5GHz 8GB) to implement the experiment.

#### 4. DEHAZING ALGORITHM

The synthetic haze image will be used as an input image to determine the image quality assessment method. It's necessary to obtain the optimum image quality assessment between the original image and the dehazed image. Hence, it can be an added value and assist in producing a quality haze-free image. In this paper, four visibility ranges are applied as a synthetic haze to the ground truth image dataset, consisting of 1km, 2km, 3km, and 4km, as listed in Table 1. These datasets will become an input to the dehazing method as in Table 2.

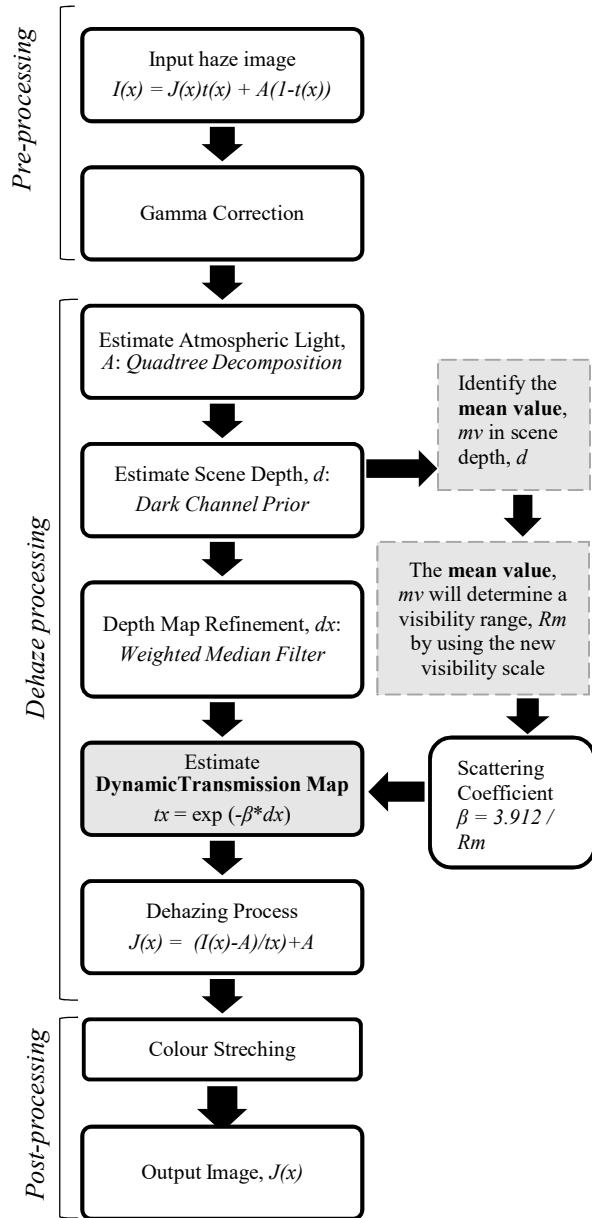


Table 2: The synthetic haze datasets with different four haze levels

Visibility Range, km	Dataset 1	Dataset 2
1 Dense haze		
2 Haze		
3 Haze		
4 Light haze		
Ground Truth		

Figure 2: The Process Flow of the Dehazing Framework

The process of the dehazing algorithm is summarized as follow:

### The proposed Dehazing algorithm

Input haze image:  $I(x)$

**Step 1:** Apply Gamma Correction to the input image

**Step 2:** Estimate airlight,  $A$  with Quadtree Decomposition of DCP

**Step 3:** Measure Scene depth with Dark Channel Prior,  $dx$

**Step 4:** Refinement depth with Weighted Median Filters

**Step 5:** Define mean value,  $mv$  from the known depth information

**Step 6:** Determine the scattering coefficient value from the  $R_m$  visibility scale,

$$\beta = 3.912 / R_m$$

**Step 7:** Estimate transmission,  $t(x) = e^{(-\beta * dx)}$

**Step 8:** Recover the scene radiance,

$$J(x) = \frac{I(x)-A}{t(x)} + A$$

**Step 9:** Post-processing with Contrast Stretching to  $J(x)$

Output scene radiance:  $J(x)$

This algorithm is shown as a procedure to implement the enhancement of dehazing algorithm with the dynamic transmission map. It applied on each different synthetic haze dataset which included light haze, moderate haze (2km and 3km) and dense haze to obtain dehazed image.

#### 4.1 Quad-tree Decomposition for airlight estimation

An input hazy image applied gamma correction to control the brightness of an image. Then, quadtree decomposition selecting a sub-block, which has the largest average value among the four divided blocks, the airlight estimate from the quad-tree subdivision is acquired repeatedly from a grey-scaled hazy picture up to a pre-specified number of times. Airlight is then chosen as an RGB-based colour vector that minimizes the Euclidean norm with (1, 1, 1) in the final block picked. Airlight is present over a large portion of the hazy picture to accurately assess airlight, and its intensity in a local area is strongest. Airlight is determined by quad-tree subdivision using a transformed image by assuming these two aspects of airlight. A grayscale image,  $L$ , is subdivided into non-overlapping blocks of size  $M/M$ , obtained from a hazy colour image,  $y$ . To mitigate adverse effects due to the brightness values of a local entity, all pixel values in each of these blocks, specified as  $L_k^{block}$ , are then replaced with their minimum quantity using Equation:

$$T_k^{block} = \min_{y \in L_k^{block}} L(y), \quad (4)$$

As a trade-off between precision and reliability, the block size  $M$  of  $64 \times 64$  was set empirically. Since the transformed image  $T$  has lower intensity values on average than the original grayscale image  $L$ , the quad-tree subdivision method will more accurately pick the candidate area to estimate the atmospheric light. After five iterations, this approach selects the sky region as the final candidate region without being interrupted by white floors in the bottom regions. The airlight can be calculated as the pixel colour vector between pixels in the final selected area, which minimizes the Euclidean norm. Airlight can be estimated more accurately by reducing the Euclidean norm [25]. To show a better result, the study of airlight estimation was performed with distinct scaled pixels as in Figure 3. It shows that the smallest pixel in airlight estimation can effectively minimize haze based on this research.



(a) 1 x 1 (b) 7 x 7 (c) 15 x 15

Figure 3: The comparison between different pixel scales to estimate airlight with quad-tree decomposition.

#### 4.2 Scene Depth Estimation

The dark channel prior is a form of haze-free outdoor image statistics. It is focused on a crucial observation - most local patches contain some very low-intensity pixels in at least one colour channel in haze-free outdoor images. We can directly estimate the thickness of the haze and retrieve a high-quality haze-free image by using this before the haze imaging model. The previous dark channel is based on the following findings on haze-free outdoor images: at least one colour channel has a very low intensity of certain pixels in most non-sky patches. A hazy picture is brighter because of the additive airlight than its haze-free equivalent, where the transmission is low. So, in regions with denser haze, the dark channel of the hazy picture is going to have a greater intensity. As follows, a dark channel defines:

$$d = \min_{y \in \Omega(x)} ( \min_{c \in \{r, g, b\}} J^c(y) ) \quad (5)$$

where  $J^c$  is an intensity for a colour channel  $c \in \{r, g, b\}$  of the RGB image, and  $\Omega(x)$  is a local patch centred at pixel  $x$ . According to Equation (5), the minimum

value among the three-colour channels and all pixels in  $\Omega(x)$  is chosen as the dark channel  $d(x)$ .

The intensity of the dark channel visually is a rough estimate of the thickness of the haze [13]. The smoothing approach used to enhance the precision of the depth map varies from many dehazing techniques. Gaussian, bilateral, soft matting, and guided filter are some of the filtering approaches used. To improve computational effectiveness, a weighted median filter [26] is used to refine the rough approximation and smooth the image. In the next segment, this property will be used for transmission estimation.

### 4.3 Dynamic scattering coefficient

The transmission map defines as Equation (2), scene depth determined with the dark channel and will calculate the transmission as Step 7:

$$t(x) = e^{-\beta(x)} \quad (6)$$

The scattering coefficient value was set up to a constant value. A more flexible model is highly desired since almost all existing single image dehazing algorithms are based on the constant hypothesis. This paper proposed a new dynamic scattering coefficient, which relied on the haze's thickness for each image. The scattering coefficient will be determined based on the mean value in-depth map estimation. To get the mean value,  $mv$  we proposed a visibility scale in the range of 0.5 meters until 10 kilometres, referred from the meteorological range in Table 5. From that range, we divided into the intensity value ( $0, I$ ) and formed a visibility scale as follows:

$$scale\ range = \frac{1}{10km - 0.05km} = \frac{1}{9.95km} = 0.1005 \quad (7)$$

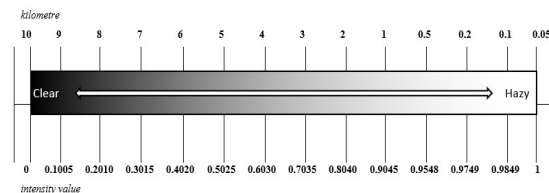


Figure 4. The proposed new visibility scales to mapping visibility range based on mean values from scene depth intensity.

The example of visibility scale mapping:

```

if {mean value} < 0.1005
    {visibility range} = 10;
elseif {mean value} < 0.2010
    .
    .
elseif {mean value} < 1
    
```

```

{visibility range} = 0.1;
elseif {mean value} >= 1
    {visibility range} = 0.05;
end
    
```

Table 3: The visibility range to its corresponding scattering coefficient

Visibility range, $R_m$	Scattering coefficient, $\beta$
1	3.9120
2	1.9560
3	1.3040
4	0.9780
5	0.7824
6	0.6520
7	0.5589
8	0.4890
9	0.4347
10	0.3912

The mean values,  $mv$  of the depth map intensity need to map this scale to determine the scattering coefficient,  $\beta$  based on the visibility range,  $R_m$  as in Table 3 as in Equation 8. The scattering coefficient will use to estimate the transmission map.

$$\beta = \frac{3.912}{R_m} \quad (8)$$

This dynamic scattering coefficient in the dehazing algorithm efficiently produces a better haze-free image because most hazy images have different haze thicknesses. This proposed method will set the parameter value based on the depth scene instead of the constant assumption. After transmission estimation, we completed the dehazing process by reversing the atmospheric scattering model in Equation (3) to obtain a haze-free image. We enhanced the result with image enhancement, which is contrast stretching to increase the image's contrast in Figure 5. The entire process of this dehazing process shown in Figure 6.



Figure 5: A comparison between contract stretching and without contract stretching

## 5. IMAGE DEHAZING RESULTS

This section is shown the process of our dehazing method to obtain the result of the haze-free image. Figure 6 show the example dataset from a hazy image, scene depth estimation, depth refinement,

transmission estimation, dehaze image and image enhancement.

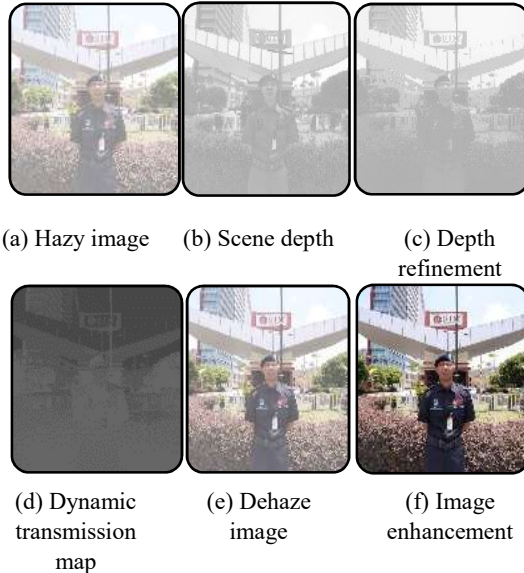


Figure 6: The steps of the dehazing process (a) Hazy image (b) Scene depth (c) Depth refinement (d) Dynamic transmission map (e) Dehaze image (f) Image enhancement

The successful of removing haze has been proved from this process. We proved this method by benchmarking our result with the ground truth image as explained in the next section.

## 6. BENCHMARK FOR COMPARATIVE ANALYSIS

The purpose of various haze conditions is to prove the dehazing algorithm, whether capable of removing haze in any hazy condition and preserving image quality. We have made the comparative analysis for the existing dehazing method, which is: Dark Channel Prior [11], Colour Attenuation Prior [17], DehazeNet [18], Haze-Line [19], and Multi-Layer Perceptron [27]. The result of these dehazing methods evaluated with standard image quality assessment [28], which are the Mean-Squared Error (MSE), Peak-Signal to Noise Ratio (PSNR) in decibel (dB) unit and Structural Similarity Index Measurement (SSIM).

Table 4 and Table 5 shows the result of dehazing methods. The Dark Channel Prior method can remove haze in all hazy levels. But, in the sky region, it looks oversaturated. Colour Attenuation Prior efficient to reduce the haze at a light hazy condition and looks natural. However, it was not successful in dense haze conditions. The resultant images still have a haze. The DehazeNet result seems perfect in removing the haze in all

conditions and quality preservation, specifically at dense haze conditions. But at the light hazy condition still was faced a disadvantage than CAP. The Haze-Line method was a bad condition, where the result looks are enhanced contrast and unnatural in all conditions. The Multi-Layer Perceptron method is useful in removing haze, but it seems to decrease the contrast of the image, which also became a bit darker. However, our proposed method shows a better value in MSE, PSNR and SSIM compared to the other method in all hazy levels. Each level of haze has been estimated with a suitable coefficient to remove haze. By using synthetic haze image, this analysis has been proved that our dehazing method able to overcome in removing haze to various haze levels.

Table 4: The result of dehazing method for random hazy images (a) Hazy Image (b) Dark Channel (c) Color Attenuation Prior (d) DehazeNet (e) Haze Line (f) MultiLayer Perceptron (g) Proposed

	1km	2km	3km	4km
DCP				
CAP				
DN				
HL				
MLP				
Own				

$$R_m = 3 \text{ Km}, R_m = 4 \text{ Km}, R_m = 4 \text{ Km}, R_m = 5 \text{ Km},$$

$$\beta = 1.3040 \quad \beta = 0.9780 \quad \beta = 0.9780 \quad \beta = 0.7824$$

a haze-free image as a benchmark, but the result shows the capability to remove haze with the suitable scattering coefficient.

Table 5: An Image Quality Assessment for First Result of Dehazing Methods

(km)	IQA	DCP	CAP	DN	HL	MLP)	Own
1	MSE	0.0071	0.0092	0.0035	0.0191	0.0056	<b>0.0002</b>
	PSNR	21.5075	20.3531	24.5885	17.1888	22.4973	<b>37.5957</b>
	SSIM	0.9230	0.9339	0.9663	0.8584	0.9540	<b>0.9964</b>
2	MSE	0.0101	0.0018	0.0015	0.0199	0.0075	<b>0.0005</b>
	PSNR	19.9742	27.3890	28.3691	17.0133	21.2236	<b>33.1622</b>
	SSIM	0.9099	0.9751	0.9740	0.8541	0.9493	<b>0.9936</b>
3	MSE	0.0111	0.0030	0.0034	0.0240	0.0076	<b>0.0008</b>
	PSNR	19.5365	25.2879	24.6757	16.1977	21.2168	<b>30.7357</b>
	SSIM	0.9042	0.9667	0.9342	0.8451	0.9449	<b>0.9901</b>
4	MSE	0.0117	0.0038	0.0047	0.0307	0.0075	<b>0.0008</b>
	PSNR	19.3360	24.1465	23.2813	15.1217	21.2335	<b>31.1194</b>
	SSIM	0.9014	0.9590	0.9096	0.8282	0.9417	<b>0.9878</b>

In addition to supporting the efficiency of this proposed dehazing method, we provided the real hazy images which referred to the Air Pollutant Index (API) value. An API value of 0 to 50, based on Table 6, means good air quality with minimal potential to affect public and environmental health. An API value of 300 to 500, on the other hand, reflects dangerous air quality with a greater potential to affect public and environmental health. To track the polluted air or the forecast, government agencies use an Air Pollutant Index (API). The concentration of each pollutant varies; API values are therefore grouped into ranges allocated to a standardized public health warning [29].

Table 6: Five Different Haze Level Condition Based on A Visible Range [41]

Category	Air Quality Index	Visibility Range (mi)	Visibility Range (km)
Good	0-50	>10	>16.1
Moderate	51-100	5-10	8.05-16.1
Unhealthy for Sensitive Group	101-150	3-5	4.83-8.05
Unhealthy	151-200	1.5-3	2.41-4.83
Very Unhealthy	201-300	1	1.61-4.83
Hazardous	300 >	<1	<1.61

The real hazy images as in Table 7 had been used as a dataset to apply our dehazing method. These datasets were captured in Malaysia outdoor scene with different API value which consisted of Moderate, Unhealthy and Very Unhealthy condition. Even these datasets were not providing

Table 7: Real-World Haze Images in Malaysia Based on the Air Pollutant Index

Date and Time	7 August 2019 4.26pm	18 Sept 2019 9.10am	19 Sept 2019 7.59am
API	51-100 Moderate (75*)	101-200 Unhealthy (188*)	201-300 Very Unhealthy (271*)
°C	32°C Broken Clouds 6km	28°C Broken clouds 2km	25°C Dense Fog 1km
Range Haze Image	8-16 km	2-5 km	1-2km
DCP			
CAP			
DN			
HL			
MLP			

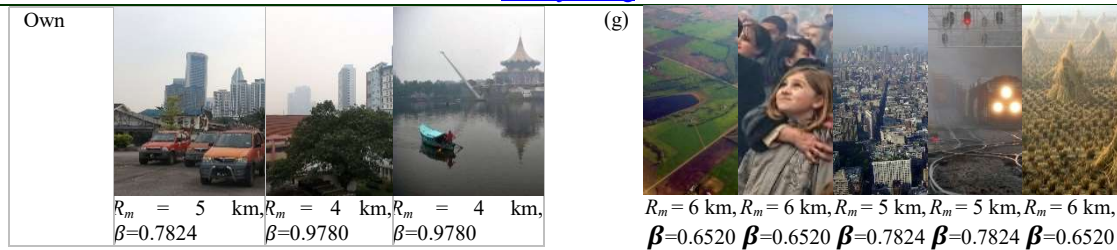
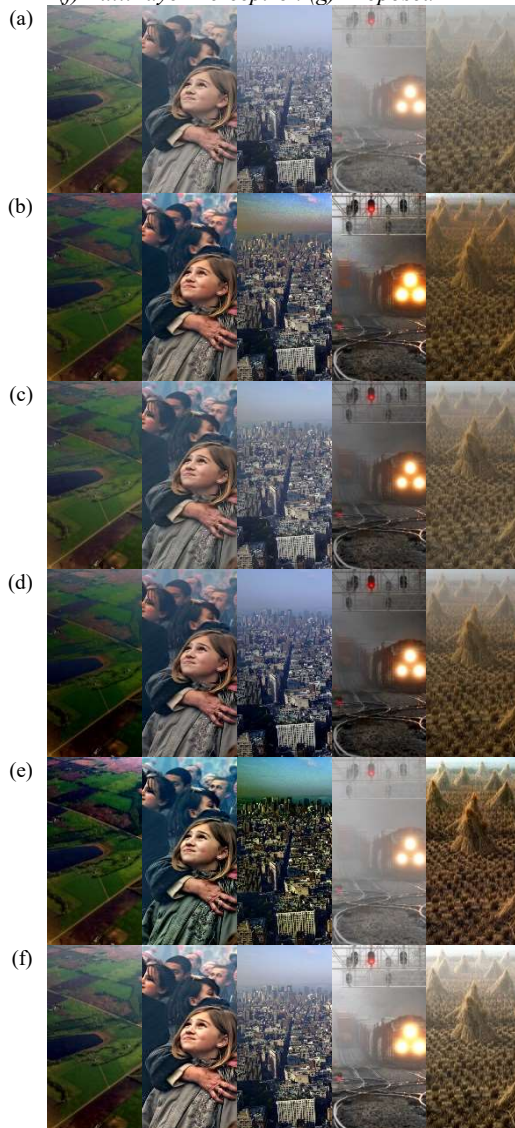


Table 8 is a dehazing result from a sample dataset in the most dehazing study. We also applied our dehazing method by using this dataset to proof the efficiency of our method.

Table 8: The result of dehazing method for random hazy images (a) Hazy Image (b) Dark Channel (c) Color Attenuation Prior (d) DehazeNet (e) Haze Line (f) MultiLayer Perceptron (g) Proposed



The result provides the estimation of the visibility range for each haze image. In various haze levels, our method was successful in removing haze for all haze levels. Besides, the enhancement method contributed to dynamic transmission by determining the suitable scattering coefficient for each level. This dynamic transmission was able to reduce issues such as over-enhanced and dense haze. Although it provides better results, this enhancement method still has a limitation if applied on indoor image and unreal haze images. Even though the proposed dehazing method managed to remove haze and produce a better result, it still needs to be improved on new proposed visibility scaling as in Figure 4. The result of the visibility range which is computed from the visibility scale seems limited in mapping the actual haze image condition.

## 7. CONCLUSION

A dehazing method is advantageous and beneficial to many applications, precisely computer vision, surveillance systems, and remote sensing. Many efforts for dehazing have been made to produce the best image quality and achieve the objective of removing the haze [30-34]. This paper proposed enhancing dehazing in a single image into four different hazy conditions based on the meteorological range. This experiment's significance is to ensure the dehazing method's efficiency in removing haze in any variety of haze and preserving the quality of the image. Simulation results compared visually and quantitatively with existing state-of-the-art schemes to verify the significance of the proposed technique. This approach will progressively be studied in future research in visibility scaling range by providing a dehazing algorithm that manages all the dehazing issues.

## ACKNOWLEDGEMENTS:

This research was funded by the Ministry of Higher Education through the Fundamental Research Grant Scheme and managed by the Research Management Centre (RMC) of University Technology Malaysia. Vot No. R.K130000.7856.5F036.

## REFERENCES:

- [1] S. G. Narasimhan and S. K. Nayar. Vision and the atmosphere. *International Journal of Computer Vision*, 48(3):233–254, 2002.
- [2] Xue, R., Zhong, M., Zhang, E., Zhao, S., & Zhang, D. & Zhang, D. (2018, June). Real-time Image Haze Removal Method for Fire Scene Images. In 2018 6th International Conference on Machinery, Materials, and Computing Technology (ICMMCT 2018). Atlantis Press.
- [3] Dong, T., Zhao, G., Wu, J., Ye, Y., & Shen, Y. (2019). Efficient Traffic Video Dehazing Using Adaptive Dark Channel Prior and Spatial-Temporal Correlations. *Sensors*, 19(7), 1593
- [4] H. Koschmieder, “Theorie der horizontalen sichtweite,” in *Beitrage zur Physik der freien Atmosphere*, 1924.
- [5] F. Cozman, and E. Krotkov. Depth from scattering. In *Proceedings of IEEE Computer Society Conference on Computer Vision and Pattern Recognition*, pages 801–806, Jun 1997.
- [6] S. G. Narasimhan and S.K. Nayar, “Contrast restoration of weather degraded images,” *IEEE Trans. on Pattern Analysis and Machine Intell.*, 2003.
- [7] Y. Y. Schechner, S. G. Narasimhan, and S. K. Nayar, “Polarization-based vision through haze,” *Applied Optics*, 2003.
- [8] J. Kopf, B. Neubert, B. Chen, M. Cohen, D. Cohen-Or, O. Deussen, M. Uyttendaele, and D. Lischinski, “Deep photo: Model-based photograph enhancement and viewing,” in *Siggraph ASIA*, *ACM Trans. on Graph.*, 2008.
- [9] R. T. Tan, “Visibility in bad weather from a single image,” in *IEEE Intl. Conf. Comp. Vision and Pattern Recog. IEEE*, 2008, pp. 1–8.
- [10] R. Fattal, “Single image dehazing,” *ACM Trans. on Graphics*, vol. 27, no. 3, p. 72, 2008.
- [11] K.He, J. Sun, and X. Tang, “Single image haze removal using dark channel prior,” *IEEE Transaction on Pattern Analysis and Machine Intelligence*, Vol. 33, no. 12, pp. 1956-1963, Dec. 2011.
- [12] J.-P. Tarel and N. Hautiere, “Fast visibility restoration from a single colour or grey level image,” in *IEEE Intl. Conf. Comp. Vision. IEEE*, 2009; pp., 2201–2208.
- [13] G. Meng, Y. Wang, J. Duan, S. Xiang, and C. Pan, “Efficient image dehazing with boundary constraint and contextual regularization,” in *Proceedings of the IEEE International Conference Computer Vision*, Washington, D.C, USA, 2013, pp. 617-624.
- [14] C. O. Ancuti and C. Ancuti, “Single image dehazing by multi-scale fusion,” *IEEE Trans. Image Proc.*, vol. 22, no. 8, pp., 3271–3282, 2013.
- [15] R. Fattal, “Dehazing using colour-lines,” *ACM Transaction on Graphics*, Vol. 34, no. 1, pp. 1–14, Nov. 2014.
- [16] K. Tang, J. Yang, and J. Wang, “Investigating haze-relevant features in a learning framework for image dehazing,” in *Proceedings of the IEEE Conference Computer Vision Pattern Recognition*, Columbus, Ohio, USA, 2014, pp. 2995–3002.
- [17] Q. Zhu, J. Mai, and L. Shao, “A fast single image haze removal algorithm using colour attenuation prior,” *IEEE Transaction Image Processing*, Vol. 24, no. 11, pp. 3522–3533, Nov. 2015.
- [18] B. Cai, X. Xu, K. Jia, C. Qing, and D. Tao, “Dehazenet: An end-to-end system for single image haze removal,” *IEEE Transaction Image Processing.*, Vol. 25, no. 11, pp. 5187–5198, Nov. 2016.
- [19] D. Berman, T. Treibitz, and S. Avidan, “Non-local image dehazing,” in *Proceedings of the IEEE Conference Computer Vision and Pattern Recognition*, Las Vegas, Nevada, USA, 2016, pp. 1674-1682.
- [20] M. Sulami, I. Geltzer, R. Fattal, and M. Werman, “Automatic recovery of the atmospheric light in hazy images,” in *Proceedings of the IEEE International Conference Computational Photography*, Santa Clara, California, USA, 2014, pp. 1-11.
- [21] Y. Bahat and M. Irani. Blind dehazing using internal patch recurrence. In *Proc. IEEE ICCP*, 2016.
- [22] D. Berman, T. Treibitz, and S. Avidan. Air-light estimation using haze-lines. In *Computational Photography (ICCP), 2017 IEEE International Conference on*, pages 1–9, 2017.
- [23] E. J. McCartney, “*Optics of the atmosphere: scattering by molecules and particles*,” New York, John Wiley and Sons, Inc., 1976.
- [24] Y. Zhang, L. Ding, G. Sharma, “HazeRD: an outdoor dataset for dehazing algorithms,” in *Proceedings of the IEEE International Conference Image Processing*, Beijing, China, 2017, pp. 3205–3209.
- [25] Dubok, et al. “Single Image Dehazing with Image Entropy and Information Fidelity.” *ICIP*. 2014, pp., 4037–4041.
- [26] Q. Zhang, L. Xu, J. Jia, “100+ Times Faster Weighted Median Filter”

- IEEE Conference on Computer Vision and Pattern Recognition (CVPR), 2014
- [27] Salazar-Colores, S., Cruz-Aceves, I., & Ramos-Arreguin, J. M. (2018). Single image dehazing using a multi-layer perceptron. *Journal of Electronic Imaging*, 27(4),0430
- [28] Z. Wang, A. C. Bovik, H. R. Sheikh, and E. P. Simoncelli, "Image quality assessment: from error visibility to structural similarity," *IEEE Trans. Image Processing*, vol. 13, no. 4, pp. 600–612, Apr. 2004.
- [29] O'Neil, S.M., Lahm, P.W., Fitch, M. J., & Broughton, M. (2013). Summary and analysis of approaches linking visual range, PM2. 5 concentrations, and air quality health impact indices for wildfires. *Journal of the Air & Waste Management Association*, 63 (9), 1083 – 1090.
- [30] Rad, A. E., Mohd Rahim, M. S., Kolivand, H., & Mat Amin, I. B. (2017). Morphological region-based initial contour algorithm for level set methods in image segmentation. *Multimedia Tools and Applications*, 76(2), 2185-2201. doi:10.1007/s11042-015-3196-y
- [31] Rakhmadi, A., Syazrah Othman, N. Z., Bade, A., Mohd Rahim, M. S., & Amin, I. M. (2010). Connected component labelling using components neighbours-scan labelling approach. *Journal of Computer Science*, 6(10), 1099-1107. doi:10.3844/jcssp.2010.1099.1107
- [32] Chaudhry, H., Rahim, M.S.M., and Khalid, A., 2018. Multi-scale entropy-based adaptive fuzzy contrast image enhancement for crowd images. *Multimedia Tools and Applications*, 77(12), pp.15485-15504.
- [33] Husain. N.A, Mohd Rahim. M.S, Kari. S, Chaudry. H (2020). "The Simulation of Synthetic Haze Based on Visibility Range for Dehazing Method in Single Image". 5th International Conference on Engineering and Technology (ICET 2020), 20-22 March 2020, Melbourne, Australia.
- [34] Husain. N.A, Mohd Rahim. M.S, Kari. S, Chaudry. H (2020). "VRHAZE: The Simulation of Synthetic Haze Based on Visibility Range for Dehazing Method in Single Image". 6<sup>th</sup> International Conference on Interactive Digital Media (ICIDM 2020), 14<sup>th</sup> – 15<sup>th</sup> December 2020, International Virtual Conference.